Investigation of Underwater Optical Wireless Communications with Turbulence

Zahra Vali[1,2], Asghar Gholami[1], Zabih Ghassemlooy[3], Masood Omoomi[1]

[1]Department of Electrical and Computer Engineering, Isfahan University of Technology, Isfahan, Iran, 8415683111
Email: z.vali@ec.iut.ac.ir, gholami@cc.iut.ac.ir, omoomi@cc.iut.ac.ir
[2]Department of Electrical and Computer Engineering, University of British Columbia, Vancouver, Canada, V6T1Z4
[3]Optical Communications Research Group, Physical and Electrical Engineering Department, Northumbria University, Newcastle Upon Tyne, UK, NE1 8ST
Email: z.ghassemlooy@northumbria.ac.uk

Abstract—**Turbulence is due to the random variations of the refractive index of the medium (in this case water), which leads to fluctuation or fading of the received light intensity. In wireless communications including underwater optical wireless communications the link performance is greatly affected. In this paper, we investigate the effect of turbulence on the probability density function (PDF) of the received light intensity. We show that lognormal and negative exponential distributions are fitted well with the PDFs of the received light intensity in weak-to-strong and saturated turbulence regimes. The goodness of fit test is performed to validate the conformity of these two distributions with the simulation results. Furthermore, we investigate the effect of the divergence angle of the Gaussian beam transmitter, the receiver's aperture diameter and field of view on the scintillation index.**

Keywords-UOWC; turbulence; PDF; lognormal; negative exponetial; scintillation index; OWC

I. INTRODUCTION

Underwater optical wireless communications (UOWC) has attracted a great deal of attentions in recent years. Using optical carriers in the blue-green wavelength bands offers higher communications bandwidth compared to the acoustic and radio frequency (RF) technologies based underwater wireless communications [1]. However, the environmental factors do greatly impact the performance of UOWC systems. The most important and well-studied environmental factors are the absorption and multiple scattering and their impacts on the performance of UOWC systems e.g., power loss, bandwidth degradation and bit error rate (BER) have been studied thoroughly [2-4].

In addition, turbulence also influences the propagating light wave and therefore affecting the UOWC link performance. The effects of turbulence in free space optical communications (FSO) have been extensively studied and reported in the literature [5]. However, in UOWC experimental investigation of turbulence effect on the link performance is more challenging, thus the focus being on system modelling and simulation [6]. A simple physical model representing a real underwater environment under different turbulence conditions based on Monte Carlo simulation, which considered all the transmitter (Tx), channel and receiver (Rx) was reported in [7]. From the two most important parameters, which determined the influence of turbulence, the refractive index variation Δn and its effect on the probability density functions (PDFs) of the received light intensity was investigated in [7]. The effect of transmission link span L on the PDFs of the received light intensity is investigated in this paper, which has not been studied yet.

Using the precise PDF of the received light intensity is important in system modeling and BER analysis. Lognormal distribution was adopted for weak and moderate turbulence regimes in [7-14]. In [11] both Gamma-Gamma and K distributions were adopted for the scintillation index (SI) values greater than 1 and a combination of exponential and lognormal distributions was used for 0.1 < SI < 1. In all these cases, the PDFs were obtained for the channel ($30\times40\times200$ cm^3) with air bubbles, which of course cannot be considered to represent a real underwater environment. Note that, performing experimental test and measurements under the strong and saturated turbulence regimes is a challenging task, therefore the focus is more on numerical and simulation investigations.

Based on the previously proposed turbulence model given in [7], in this paper we investigate the fluctuations of the received light intensity for a range of link spans and predict its PDF under the weak-to-strong and saturated turbulence regimes. Furthermore, we investigate the SI by considering the divergence angle of the Gaussian beam Tx and the Rx's aperture diameter as well as its field of view (FOV).

The rest of the paper is organized as follows. The proposed PDF distributions are described in section II. Simulation results are discussed in section III and section IV concludes the paper.

II. PDF DISTRIBUTIONS

Turbulence in atmosphere is categorized as weak, moderate, strong and saturated based on its strength [15]. Up to now there is no comprehensive single mathematical model for turbulence, because of the complex nature of the environment. The three most widely adopted PDF distributions of the received light intensity in FSO for the weak, weak-to-strong and saturated regimes are lognormal, Gamma-Gamma and negative exponential, respectively. In this work, both lognormal and negative exponential distributions are considered. The lognormal distribution of the received light intensity I is given by [16]:

$$p(I) = \frac{1}{I\sigma_I\sqrt{2\pi}} \exp\left\{ -\frac{\left[\ln(\frac{I}{I_0}) + \frac{1}{2}\sigma_I^2\right]^2}{2\sigma_I^2} \right\}, \ I > 0 \ (1)$$

where I_0 is the mean received light intensity and σ_I^2 is the SI, which is given as:

$$\sigma_I^2 = \frac{\langle I^2 \rangle - \langle I \rangle^2}{\langle I \rangle^2}. \quad (2)$$

The negative exponential distribution is given by [15]:

$$p(I) = \frac{1}{I_0}\exp(-\frac{I}{I_0}), \ I > 0. \quad (3)$$

III. Simulation Results

A. PDF Distributions

The model used in [7] was based on the interaction of propagating photons with the consecutive turbulent cells with different refractive indices and sizes, see Fig. 1. Turbulent cells are defined with consecutive layers with a width Δz on the z-axis. The curved boundaries with the radius R_i and a normal vector $\vec{n}_i = (\sin\theta_i \cos\varphi_i, \sin\theta_i \sin\varphi_i, \cos\theta_i)$ separate the adjacent layers. By choosing θ_i and φ_i randomly, rotation of curved boundaries along the z axis is implied. Note, θ_i is the polar angle chosen randomly between zero and θ_{max} and φ_i is the radial angle chosen randomly within the range of [0, 2π] with a uniform distribution. Δn and L are the two important factors to affect the strength of turbulence as in [7]. Here we fix Δn to 80e-5 and consider the effect of L on the PDF of the received light intensity. All the key system parameters are listed in Table 1. For more information on system parameters refer to [7].

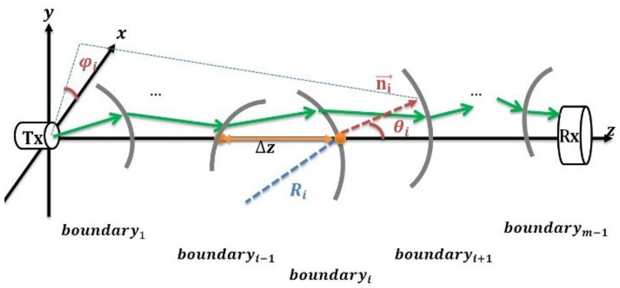

Figure 1. A schematic diagram of the system consisting of Tx, turbulent channel and Rx

Fig. 2 shows the PDF of the simulated received light intensity against the normalized intensity fitted with lognormal and negative exponential distributions for a range of L and SI. Note that, the total number of received photons at the Rx for all 1e3 channel realizations were normalized to the average intensity I_0 and the SI values were obtained from (2). As shown there is a good fit between the lognormal and negative exponential distributions and the simulation results for the weak-to-strong and saturated turbulence regimes, respectively. Note, other reported turbulence PDF distributions for strong atmospheric turbulence e.g., lognormal-rician, I-K, K and Gamma-Gamma distributions all tend to negative exponential distribution therefore, are not considered here [15].

TABLE I. Model Parameters

Section	System Parameters	
	Parameter	***Value***
Tx	Number of Transmitted Photons	1e4
	Wavelength	520 nm
	Beam Divergence Angle (Half Angle)	0.00075 rad
	RMS Beam Width	15 mm
Rx	Aperture Diameter	100 mm
	Aperture FOV	180°
Underwater Channel	Link Span	30, 40, 80, 120, 150 m
	Number of Channel Realizations	1e3
	Δn	80e-5
	Δz	50 cm
	θ_{max}	45°

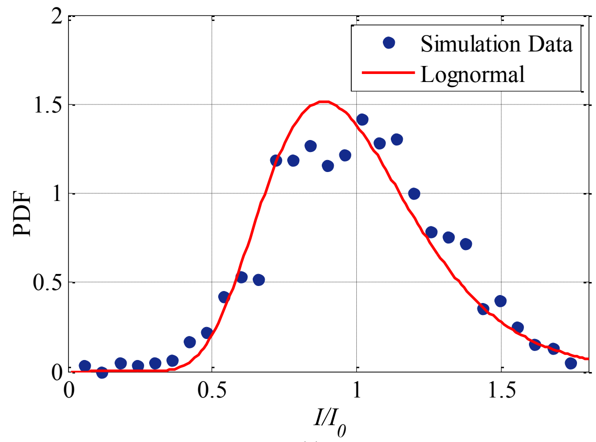

(a)

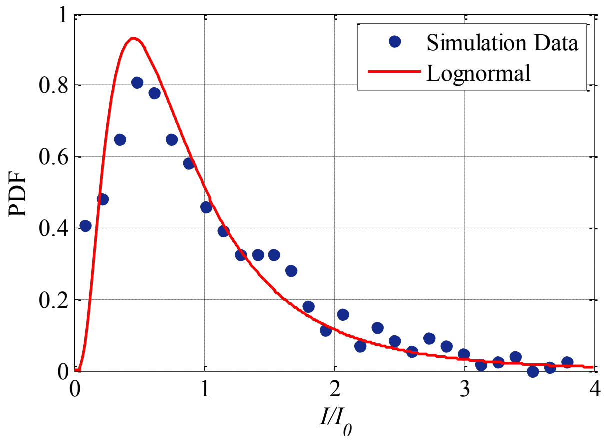

(b)

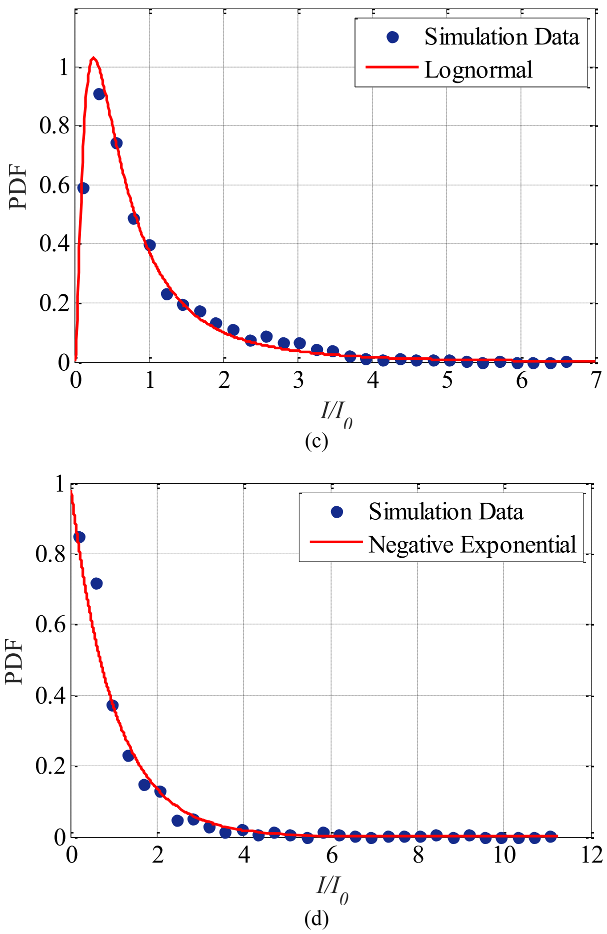

Figure 2. PDF of the simulated received light intensity vs. the normalized intensity fitted with lognormal and negative exponential distributions for: (a) L = 40 m and SI=0.08 (b) L = 80 m and SI=0.52 (c) L = 120 m and SI=0.9, and (d) L = 150 m and SI=1.40

TABLE II. R^2 VALUES

PDF	R^2	SI
Lognormal	0.8762	0.08
	0.8211	0.52
	0.9891	0.9
Negative Exponential	0.9751	1.40

B. Goodness Of Fit (GOF) Test

To evaluate how well the PDFs of simulation results fit with the lognormal and negative exponential distributions, we determine the coefficient of determination R^2 as given by [17]:

$$R^2 = 1 - \frac{\sum_{i=1}^{N}(x_i - y_i)^2}{\sum_{i=1}^{N}(x_i - \bar{x})^2} \quad (4)$$

where, N is the number of bins in the simulation distribution, x_i and y_i are the simulated and predicted values for the i^{th} intensity bin, respectively and $\bar{x}$ is the average of x_i. Generally 0 < R^2 < 1, where the upper value i.e., 1 indicates a close fit between the simulation results and the lognormal and negative exponential distributions. Table II shows R^2 and SI for all cases.

C. SI Variations

In addition to L and Δn, we also consider the divergence angle of the Gaussian beam Tx and Rx's aperture diameter as well as FOV impact on the SI. Fig. 3 shows the SI variations as a function of the Tx's divergence angle for a range of Δn and for L = 30 m. As depicted in Fig. 3, SI increases with Δn. For lower values of the divergence angles, the transmitted beam illuminates the center of the Rx (i.e., photodetector surface) and due to aperture averaging the turbulence effect is low. However, the SI increases with the divergence angle due to more beam spreading and beam wandering and then reaches the saturated levels. In this state, the beam width is wider than the Rx's area and the beam wandering effect reduces thus resulting in reduced SI.

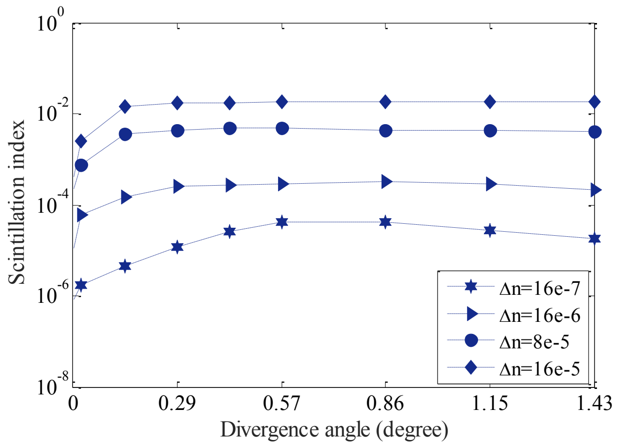

Figure 3. SI vs. Tx's divergence angle for different values of Δn and for L = 30 m

Fig. 4 shows the SI variations as a function of the Rx's aperture diameter for different values of Δn and for L = 30 m. As shown the SI decreases with the aperture diameter increase for all values of Δn. Increasing the aperture diameter by ten times results in reduced SI by 100 times. Mitigating the random fluctuations of the received light intensity by increasing the aperture area is known as aperture averaging which compensates for the scintillation and beam wander effects [18]. It should be noted that, increasing the aperture area will also increase the background noise, thus leading to lower signal to noise ratio which is not considered here.

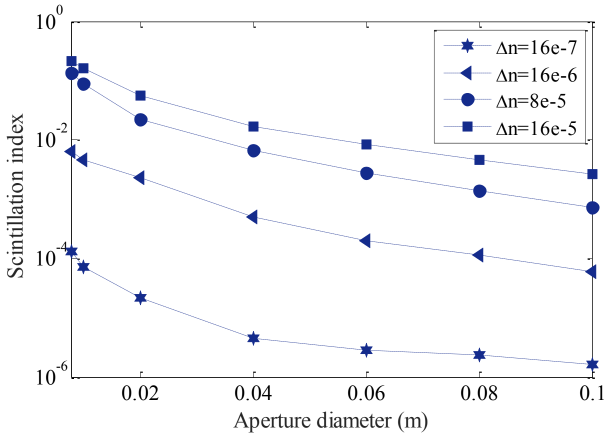

Figure 4. SI vs. Rx's aperture diameter for different vlaues of Δ*n* and *L* = 30 m

Finally, Fig. 5 illustrates the variation of SI against the Rx's FOV for different values of Δ*n* and for *L* = 30 m. The effect of turbulence on the fluctuations of the angle of arrival of photons at the Rx is negligible. Therefore, increasing the Rx's FOV has negligible effect on the SI except for the FOV < 1˚. For lower values of Δ*n*, the effect of the FOV increase on SI is negligible since the angular spreading at the Rx is less. However, for higher values of Δ*n*, it is more significant. E.g., for Δ*n* = 80e-5, increasing the FOV by ten times results in reducing the SI by 14.8 times.

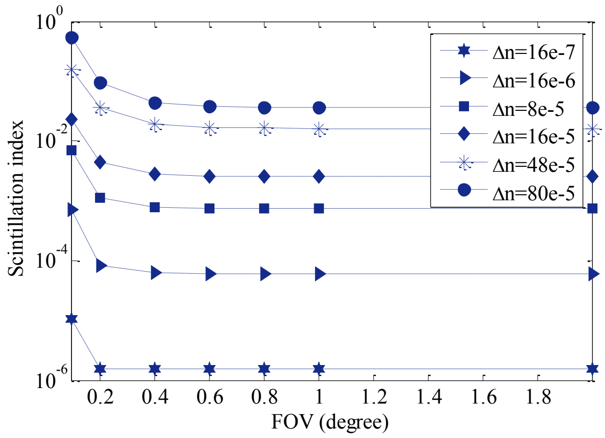

Figure 5. SI vs. Rx's FOV for different vlaues of Δ*n* and *L* = 30 m

IV. CONCLUSION

Link span is one of the main factors affecting the turbulence strength and hence the fluctuations of the received light intensity. Based on our previously proposed turbulence model, we investigated the effect of link span up to 150 m on the PDF of the received light intensity while the water refractive index variation was the same in all cases. Simulation results showed that lognormal and negative exponential distributions fitted well with the PDF of the received light intensity for weak-to-strong and saturated turbulence regimes, respectively. Performing GOF test, it was shown that the two mentioned distributions predict the simulation results well. In addition, the effect of the Tx's divergence angle, Rx's aperture diameter and FOV on SI were investigated. It was shown that while the SI variations with the Tx's divergence angle depends on the refractive index variation, increasing the Rx's aperture diameter and FOV reduce the SI.

REFERENCES

[1] Z. Zeng, A survey of underwater wireless optical communication, University of British Columbia, 2016.

[2] C. Gabriel, M. A. Khalighi, S. Bourennane, P. Léon, and V. Rigaud, "Monte-Carlo-based channel characterization for underwater optical communication systems," Journal of Optical Communications and Networking, vol. 5, pp. 1-12, 2013.

[3] S. Tang, Y. Dong, and X. Zhang, "Impulse response modeling for underwater wireless optical communication links," IEEE Transactions on Communications, vol. 62, pp. 226-234, 2014.

[4] Z. Vali, A. Gholami, D. G. Michelson, Z. Ghassemlooy, M. Omoomi, and H. Noori, "Use of Gaussian beam divergence to compensate for misalignment of underwater wireless optical communication links," IET Optoelectronics, vol. 11, pp. 171-175, 2017.

[5] Z. Nazari, A. Gholami, Z. Vali, M. Sedghi, and Z. Ghassemlooy, "Experimental investigation of scintillation effect on FSO channel," 24th Iranian Conference on Electrical Engineering (ICEE), pp. 1629-1633, 2016.

[6] J. R. Potter, "UComms: a conference and workshop on underwater communications, channel modeling, and validation," IEEE Journal of Oceanic Engineering, vol. 38, pp. 603-613, 2013.

[7] Z. Vali, A. Gholami, Z. Ghassemlooy, D. G. Michelson, M. Omoomi, and H. Noori, "Modeling turbulence in underwater wireless optical communications based on Monte Carlo simulation," Journal of the Optical Society of America A, vol. 34, pp. 1187-1193, 2017.

[8] M. P. Bernotas, and C. Nelson, "Probability density function analysis for optical turbulence with applications to underwater communications systems," in Proc. of SPIE, vol. 9827, pp. 98270D-98270D-10, 2016.

[9] W. Liu, Z. Xu, and L. Yang, "SIMO detection schemes for underwater optical wireless communication under turbulence," Photonics Research, vol. 3, pp. 48-53, 2015.

[10] M. V. Jamali, F. Akhoundi, and J. A. Salehi, "Performance characterization of relay-assisted wireless optical CDMA networks in turbulent underwater channel," IEEE Transactions on Wireless Communications, vol. 15, pp. 4104-4116, 2016.

[11] M. V. Jamali, P. Khorramshahi, A. Tashakori, A. Chizari, S. Shahsavari, S. AbdollahRamezani, et al., "Statistical distribution of intensity fluctuations for underwater wireless optical channels in the presence of air bubbles," Iran Workshop on Communication and Information Theory (IWCIT), pp. 1-6, 2016.

[12] Z. Vali, A. Gholami, D. G. Michelson, Z. Ghassemlooy, M. Omoomi, and H. Noori, "Monte Carlo simulation of underwater wireless optical communications in turbulent environments," IEEE AP-S Symposium on Antennas and Propagation and USNC-URSI Radio Science Meeting, San Diego, California, USA, 2017.

[13] A. C. Boucouvalas, K. P. Peppas, K. Yiannopoulos, and Z. Ghassemlooy, "Underwater optical wireless communications with optical amplification and spatial diversity," IEEE Photonics Technology Letters, vol. 28, pp. 2613-2616, 2016.

[14] S. A. Arpali, Y. Baykal, and Ç. Arpali, "BER evaluations for multimode beams in underwater turbulence," Journal of Modern Optics, vol. 63, pp. 1297-1300, 2016.

[15] Z. Ghassemlooy, W. Popoola, and S. Rajbhandari, Optical wireless communications: system and channel modelling with Matlab, CRC press, 2012.

[16] L. C. Andrews, R. L. Phillips, and C. Y. Hopen, Laser beam scintillation with applications, vol. 99, SPIE press, 2001.

[17] I. E. Lee, Free space optical communication systems with a partially coherent Gaussian beam and media diversity, Northumbria University, 2014.

[18] A. K. Majumdar, and J. C. Ricklin, Free-space laser communications: principles and advances, vol. 2, Springer Science & Business Media, 2010.